Impact of tellurite-based glass structure on Raman gain

Guillaume Guery [a,b,c,*], Alexandre Fargues [a], Thierry Cardinal [a], Marc Dussauze [b], Frederic Adamietz [b], Vincent Rodriguez [b], John David Musgraves [c], Kathleen Richardson [c], Philippe Thomas [d]

[a] CNRS, Université de Bordeaux, ICMCB, 87 avenue du Dr. A. Schweitzer, Pessac F-33608, France
[b] Institut des Sciences Moléculaires, CNRS UMR 5255, Université de Bordeaux, 33405 Talence, France
[c] School of Materials Science and Engineering, COMSET, Clemson University, Clemson, SC 29634, USA
[d] Laboratoire Science des Procédés Céramiques et de Traitements de Surface, UMR 6638 CNRS, Centre Européen de la Céramique, 12 rue Atlantis, 87068 Limoges Cedex, France

ARTICLE INFO

ABSTRACT

Raman gain efficiency and structure of tellurite glasses in the $TeO_2–TaO_{5/2}–ZnO$ system have been investigated by Raman and IR spectroscopies. It has been found that replacement of $TaO_{5/2}$ by ZnO does not significantly modify the respective proportion of TeO_4, TeO_3 and TeO_{3+1} entities but induces an important decrease of the TeO_4 structural units Raman cross section. Change of the glass structure at the middle range length scale is proposed to be at the origin of the large decrease of the Raman cross section of the TeO_4 units.

© 2012 Elsevier B.V. All rights reserved.

1. Introduction

In high-speed optical communications, new materials which can sustain increased information flow (short and long distance networks) for a more efficient use of available communication channels and for an access to new spectral bandwidth are of interest. Tellurite oxide-based glasses are excellent candidates for these applications due to their broad transmission range (0.3–5 μm) and their high Raman cross section as compared to existing commercial fibers materials [1]. Tellurite-based glasses appear to be promising candidates for next generation broadband and high-gain Raman amplifiers. Indeed, an exceptional Raman gain to around 58 times that of fused silica has been already measured in such materials [2]. Raman gain responses are usually evaluated by measuring the Raman spontaneous response [3]. The vibrational glass response depends both on glass composition and excitation wavelength. Raman spectrum collected for excitation near the band edge, gives rise to important dispersion in term of intensity and modification of Raman spectrum for multicomponent glasses [4]. Indeed, pure TeO_2 glass is hardly possible to prepare. Previous investigation has shown that the introduction in tellurite of d^0-transition ions (W^{6+}, Nb^{5+}, Ta^{5+}, Ti^{4+}, etc.) or ions with a lone pair of electrons such as Tl^+ or Pb^{2+} allows maintaining a high optical nonlinearity, high Raman gain and improve the processing technology [2,5,6]. Introduction of metal oxide such as ZnO or/and alkali an alkaline earth have been also reported to lead to suitable glasses for optical fiber fabrication [7,8]. The investigation on the effects of the introduction of various oxide compounds on the tel-lurite network, on the Raman gain response and on the resulting spectral bandwidth have been investigated by different research groups. Correlation between the glass structure/tellurium oxide polyhedra and the Raman response are discussed [8]. The spectral modifications have been attributed to different ratio of TeO_4 disphenoids units and TeO_3 molecular entities. The nature of the oxide introduced in the tellurite network affects this ratio but the resulting effect on both Raman spectral shape and Raman intensity are not fully understood.

Tantalum tellurite glass family has already been investigated [9,10] and proposed as good candidate for Raman gain. In the present study, thermal, physical and structural properties of glasses in the $TeO_2–TaO_{5/2}–ZnO$ glass system have been investigated. Among the d^0 transitions ions, tantalum offers wide bandgap energy which guaranties a low resonant vibrational contribution to the Raman response for excitation in the visible and in the near infrared range and high polarizability. ZnO has been introduced as a glass modifier to improve the thermal stability properties of the glass to resist crystallization tendencies [11]. This Letter aims to point out the importance of measuring Raman cross section for evaluating the influence of the glass modifier on the magnitude of the Raman response.

2. Experimental procedures

Tellurite-based glasses in the host system $TeO_2–TaO_{5/2}–ZnO$ were prepared in 7 g batches. The glasses were prepared from high purity elements (TeO_2 99.99% (Alfa Aesar), $TaO_{5/2}$ 99.993% (Alfa Aesar) and ZnO 99.0% (Alfa Aesar)). Before melting, raw materials were pre-heated at 200, 300 and 400 °C to eliminate or minimize components such as water, hydroxyl and carbonyl groups, respec-

* Corresponding author at: CNRS, Université de Bordeaux, ICMCB, 87 avenue du Dr. A. Schweitzer, Pessac F-33608, France.
E-mail address: gguery@clemson.edu (G. Guery).

tively. The batch mixtures were melted in a platinum crucible at a temperature between 800 and 1000 °C, depending on the glass composition, for 15 min to prevent volatilization. Then, the glass were quenched on a pre-heated brass plate and annealed overnight at a temperature 40 °C below the glass transition temperature (T_g). Glass compositions and glass homogeneity were checked by Elemental Dispersive Spectroscopy (EDS). The X-ray Diffraction (XRD) has been performed to confirm the amorphous state.

Characteristic temperatures such as glass transition temperature (T_g), onset of crystallization (T_x) and crystallization temperature (T_p) were determined by Differential Scanning Calorimetry (DSC) using a heating rate of 10 °C/min from room temperature to 550 °C on a commercial DSC apparatus (Netzsch DSC 404). The measurements were carried out in hermetically sealed aluminum pans.

Bulk glass material densities were measured by Archimede's principle using diethylphtalate liquid. The accuracy was better than 0.3%.

Linear refractive indices were measured using the Brewster's angle method at a wavelength of 752 nm. The recorded signal was fitted using Fresnel equations. The experimental error was found to be ±0.005 refractive index units (RIU).

The IR spectra were recorded on a Nexus 670 spectrophotometer (Thermo Optek) equipped with a DTGS detector and a germanium coated KBr beam splitter or hybrid FIR beam splitter. A total of 200 scans were averaged with a resolution of 4 cm^{-1}. The spectrometer was purged with dry air to minimize atmospheric CO_2 and water vapor. Reflectance experiments were performed using an external reflection attachment (Graesby, Specac) at an angle of incidence of 12°. The complex refractive index of each sample was obtained through Kramers–Krönig analysis of its specular reflectance spectrum [12,13]. The infrared spectra reported in this Letter are in the form of $v \cdot \varepsilon''$, where v (in cm^{-1}) is the infrared wavenumber, and ε'' is the imaginary part of the dielectric constant function calculated from the relation $\varepsilon'' = 2 \cdot n \cdot k$ where $n(v)$ and $k(v)$ are the real and imaginary parts of the complex refractive index, respectively.

In order to estimate the spontaneous Raman cross section of different tellurite glasses, polarized (VV) spontaneous Raman spectra of the vitreous materials were measured using a micro-Raman set-up with an excitation wavelength of 752 nm. A 100× microscope objective, with a numerical aperture of 0.75, was used to focus the light on the front polished surface of the sample. Combination of polarizers was used to select the polarization direction (vertical V and/or horizontal H) of the backscattered light. The scattered light was collected and spectrally analyzed with a CCD detector mounted on the exit port of a single grating spectrograph, with a typical resolution of about 6 cm^{-1}. The Rayleigh line was suppressed with a holographic notch fiber. The Raman gain coefficient g_R (m/W) is calculated from spontaneous Raman scattering spectra in vertically polarized (VV) scattering geometry after application of corrective factors and by scaling the Raman response to well-characterized standards, i.e. fused-silica and Schott SF6 glasses [14]. A near infrared excitation wavelength (at 785 nm) was chosen to insure an excitation energy well below the band gap region for tellurite samples.

3. Results

Table 1 summarizes the glass composition analyzed, their characteristic temperatures (glass transition T_g, onset of crystallization T_x, crystallization temperatures T_p), glass stability ($\Delta T = T_x - T_g$) and the glass volumetric weight. Note that in the TeO_2–$TaO_{5/2}$ binary system, the glass transition temperature, the temperature of onset of crystallization and the density increase when the $TaO_{5/2}$ content increases. All the materials in the binary and the ternary glass system exhibit a remarkable behavior against crystallization, thanks to a $\Delta T > 100$ °C except for $90TeO_2$–$10TaO_5$. In $80TeO_2$–$(20-x)TaO_{5/2}$–$xZnO$ glass system, the glass transition temperature, the onset of crystallization, the crystallization temperature and the density decrease during the substitution of $TaO_{5/2}$ for ZnO.

Table 2 summarizes the measured refractive indices which evolution can be correlated to the number density of Te atoms for each glass compositions. As it can be observed, the refractive index remains constant with the variation of tantalum oxide content. It shows that the decrease of tellurium oxide content is compensated in term of polarizability by the addition of tantalum oxide. This observation could be related to the relatively high polarizability of the Ta–O bonds [15]. At the inverse, the refractive index is dependent on the ZnO content and a decrease of 6×10^{-2} is observed as zinc oxide replaced $TaO_{5/2}$ in this glass system. In a first approximation, this significant decrease could be related to the

Table 1
T_g glass transition temperature, T_x onset of the crystallization peak, T_p maximum of the crystallization peak, ΔT glass stability and volumetric weight.

Glass composition	T_g (±2 °C)	T_x (±2 °C)	T_p (±2 °C)	$\Delta T = T_x - T_g$	Volumetric weight (±0.3% g/cm^3)
$90TeO_2$–$10TaO_{5/2}$	351	430	465	79	5.81
$85TeO_2$–$15TaO_{5/2}$	370	489	516	119	5.91
$80TeO_2$–$20TaO_{5/2}$	387	502	505	115	5.99
$80TeO_2$–$15TaO_{5/2}$–$5ZnO$	360	496	537	136	5.89
$80TeO_2$–$10TaO_{5/2}$–$10ZnO$	350	478	526	128	5.78
$80TeO_2$–$5TaO_{5/2}$–$15ZnO$	335	468	498	133	5.67

Table 2
n Refractive indices, number density of Te atoms, area of relative Raman gain peak and relative Raman gain as a function of $TaO_{5/2}$ and ZnO contents.

Glass composition	n (752 nm) (±0.05)	Number density of Te atoms ($\times 10^{27}$ mol/m^3)	Area of relative Raman gain deconvoluted peak ($\times 10^{-16}$ m/W.cm^{-1})	Relative Raman gain to SiO_2 measured at 660 cm^{-1}
$90TeO_2$–$10TaO_{5/2}$	2.15	18.99	1.794	37.2
$85TeO_2$–$15TaO_{5/2}$	2.15	17.92	1.868	38.2
$80TeO_2$–$20TaO_{5/2}$	2.14	16.79	1.698	31.1
$80TeO_2$–$15TaO_{5/2}$–$5ZnO$	2.12	17.21	1.388	27.8
$80TeO_2$–$10TaO_{5/2}$–$10ZnO$	2.08	17.63	1.177	23.3
$80TeO_2$–$5TaO_{5/2}$–$15ZnO$	2.06	18.10	0.902	18.5

lower polarizability of the Zn–O bonds as compared to Te–O and Ta–O bonds.

Figures 1 and 2 show, respectively, the IR and Raman spectra of the studied glasses. In Raman, the magnitude of the Raman signal collected for all spectra has been corrected in order to access to the relative Raman cross section and then to the estimation of the Raman gain following the procedure defined by Rivero et al. and Dai et al. [4,16]. The two series of composition exhibit very similar IR and Raman spectra, with an intense band picking at $610 \, \text{cm}^{-1}$ in IR and $660 \, \text{cm}^{-1}$ in Raman, a shoulder at higher wavenumber (≈ 720–$830 \, \text{cm}^{-1}$ in both IR and Raman) and a large and intense envelope at lower wavenumber with an apparent maximum at $300 \, \text{cm}^{-1}$ in IR and $450 \, \text{cm}^{-1}$ in Raman.

In a first approach, a global assignment of these vibrational modes can be proposed based on previous studies on pure TeO_2 crystalline phases (α-TeO_2, β-TeO_2 and γ-TeO_2) [17–19] and TeO_2 glasses and crystals containing various modifier oxides [8,20–22]. Lets remind that the coordination state of tellurium atoms in TeO_2 is a TeO_4 trigonal bipyramidal disphenoids (tbp). In α and β crystalline phase, each TeO_4 entities are connected through highly asymmetric bridges Te–$_{ax}O_{eq}$–Te where ax. and eq. notation corresponds to axial and equatorial oxygens of the TeO_4 tbp structural units. At the inverse the γ-TeO_2 lattice contains both very asymmetric and much more symmetric Te–O–Te linkage. When cations modifier are introduce within the TeO_2 matrix, structural variations are interpreted by a progressive transformation of TeO_4 units to TeO_3 units, via the intermediate state TeO_{3+1} corresponding to a distorted TeO_4 entity with one long Te–O bond, as found in TeO_2 crystals and some binary tellurite crystals [23]. Finally, the vibrational modes observed in our study can be associated with these different structural elements as follows: The bands located at $610 \, \text{cm}^{-1}$ (mainly IR active) and at $660 \, \text{cm}^{-1}$ (mainly Raman ac-
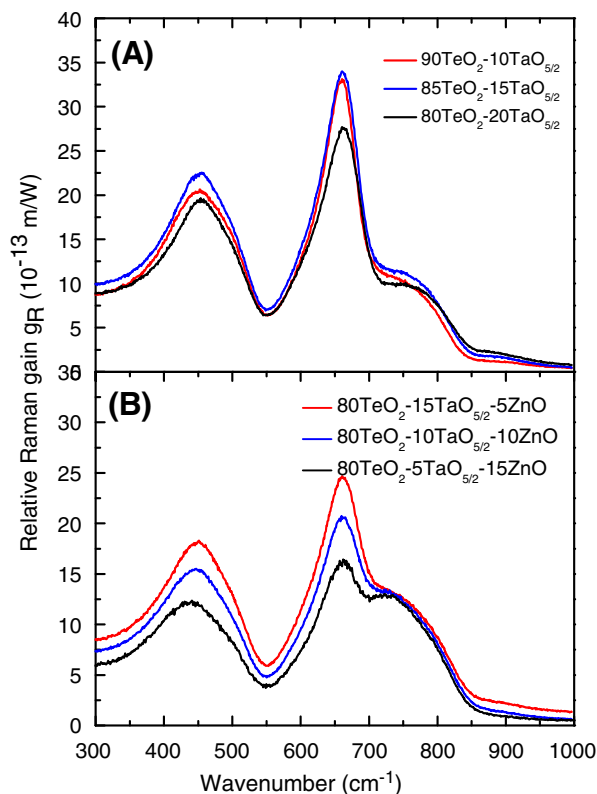
Figure 2. Raman spectra of bulk glass systems $(100-x)TeO_2$–$xTaO_{5/2}$ in (A) and $80TeO_2$–$(20-x)TaO_{5/2}$–$xZnO$ in (B) depicted in the form of relative Raman gain using pure SiO_2 as reference.

tive) originate, respectively from anti-symmetric and symmetric stretching of TeO_4 units forming a continuous network. The high energy broad shoulder (720–$830 \, \text{cm}^{-1}$) is expected to contain at least two main contributions generally assigned to stretching modes of TeO_{3+1} and TeO_3 units, as the main Raman and IR band in $M^{2+}(TeO_3)^{2-}$ oxide is located in the range 700–$750 \, \text{cm}^{-1}$ which maximum position depends on the nature of counter cations. However, it is also expected in this region some low intensity vibration modes originating from TeO_4 entities in a pure Tellurite network [17,18]. At lower wavenumber, the band at $450 \, \text{cm}^{-1}$ active in both IR and Raman and the band at $300 \, \text{cm}^{-1}$ mainly active in IR result from highly coupled bending and stretching modes of continuous chains Te–O–Te of corner sharing TeO_4, TeO_{3+1} and TeO_3 polyhedra. One should also expect in our compositions a weak band at $890 \, \text{cm}^{-1}$ due to the TaO_n stretching vibrations [24].

In the binary system, the variation of the tantalum oxide content (from 10% to 20%) does not induce significant spectral variation. In both IR and Raman spectra, the maximum of the high frequency shoulder is slightly shifted and minor variations appear in the low frequency region. These data tend to show that the introduction of Ta^{5+} cations in the TeO_2 matrix does not influence considerably the tellurite network. In the ternary system, the IR spectra show a slight increase in the region of TeO_{3+1}/TeO_3 stretching and a continuous increase of the low frequency mode. The Raman spectra exhibit a large gradual decrease of the two main bands at 450 and $660 \, \text{cm}^{-1}$, both linked to a TeO_4 constituted network. Thus, both IR and Raman spectral variations can be described as a partial depolymerization of the glass network inducing an increase of TeO_{3+1}/TeO_3 units. However, one should notice that the spectral variations observed are at least four times more pronounced in the Raman data as compared to the IR spectra.
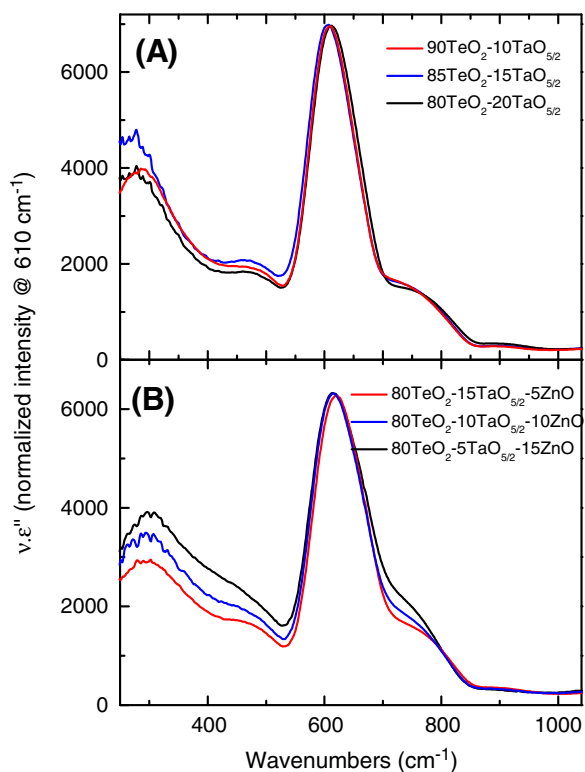

Figure 1. Infrared ($v^*\varepsilon''$) spectra obtained from Kramers–Kronig transformed specular reflection spectra of bulk glasses in the systems $(100-x)TeO_2$–$xTaO_{5/2}$ in (A) and $80TeO_2$–$(20-x)TaO_{5/2}$–$xZnO$ in (B).

Concerning the Raman gain data estimated by the spontaneous Raman scattering measurements, one should first notice that the volume concentration of Te^{4+} decreases by only 10% between the glass composition $80TeO_2$–$20TaO_{5/2}$ and $80TeO_2$–$5TaO_{5/2}$–$15ZnO$ (Table 2). Reporting the value of the Raman gain, the magnitude in the binary glass system is fairly constant; however, in the ternary glass system, with the introduction of ZnO in the glass network the Raman gain value is divided by 2 between the glass compositions $80TeO_2$–$20TaO_{5/2}$ and $80TeO_2$–$5TaO_{5/2}$–$15ZnO$. In a second step, in order to fully take into account the relative importance of the different structural units a decomposition of the relative Raman gain spectra into Gaussian function have been performed, accordingly to the assignment of the bands described above. The decomposition obtained for the glass composition $80TeO_2$–$(20-x)TaO_{5/2}$–$xZnO$ is shown as an example in Figure 3. A band at 349 cm^{-1} has been introduced for all spectra to take into account the low frequency contribution not discussed in this paper. Above 400 cm^{-1}, seven Gaussians have been used to decompose the Raman spectra accordingly to the spectral assignments detailed above. In the table in insert are reported the band position and the bandwidth which have been fixed for all glass composition. A maximum shift of 2% of the position of the band located around 450 cm^{-1} has been constrained between the different spectra. Spectral decompositions were obtained by adjusting only the magnitude of the different vibration bands. As shown in the Figure 4, reporting the Raman cross section for each contribution after decomposition, when the ZnO concentration decreases only two vibrations are mainly affected: the vibration at around 445 cm^{-1} and the vibration at around 658 cm^{-1} respectively attributed to Te–O–Te bending and symmetric stretching of TeO_4 units. The variation of magnitude is well above the estimated precision of the measurement which is 10%. The intensity associated to the vibrations associated to TeO_{3+1}/TeO_3 (band at 726 and 789 cm^{-1}) is stable. Only for the glass composition $80TeO_2$–$20TaO_{5/2}$ a lowest magnitude of the band at 726 cm^{-1} is observed.

4. Discussion

According to the Raman spectra and the decomposition into Gaussian function, as the zinc oxide is introduced in the $80TeO_2$–
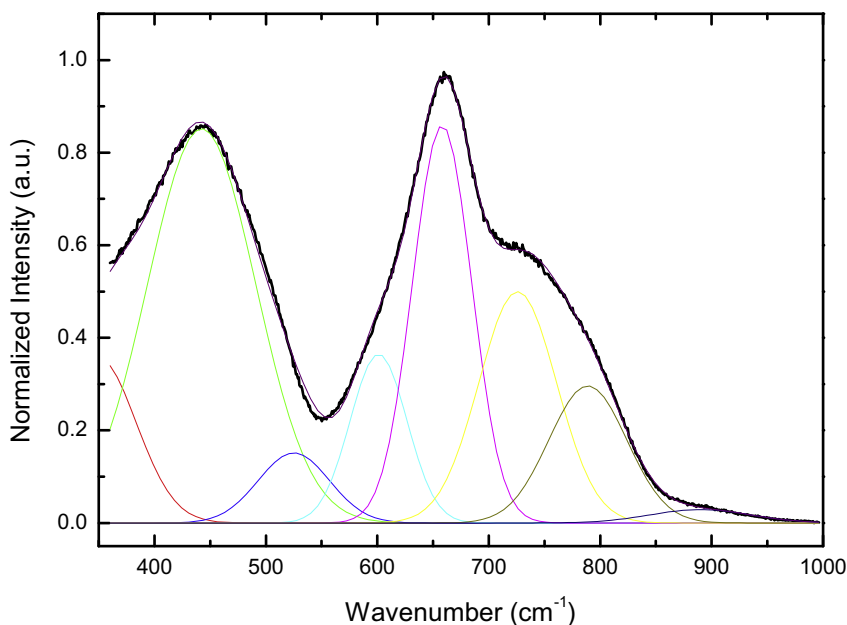

Figure 4. Evolution of the Raman cross section for $80TeO_2$–$(20-x)TaO_{5/2}$–$xZnO$ glass system.

$(20-x)TaO_{5/2}$–$xZnO$ glass system, the magnitude of intensity of the bands related to TeO_4 and Te–O–Te vibrations strongly decreases. The intensity of the Raman response associated to the TeO_{3+1} and TeO_3 vibrations at around 726 and 789 cm^{-1} remains almost constant among the different glass composition taking into account the accuracy of the measurement which is 10% in relative value. As the volume concentration of Te^{4+} has rather a smooth evolution with variation lower than 10%, the evolution of Raman intensity associated to the TeO_4 polyhedrons should be related either to a decrease of the number of TeO_4 units or to a decrease of the Raman cross section associated to those structural entities. A decrease of the number of TeO_4 units should be linked to an increase of the number of TeO_{3+1} or TeO_3 entities. Such evolution cannot be clearly discerned in Raman where the intensity of the mode due to TeO_{3+1} and TeO_3 remain unchanged. Moreover, accordingly to the infrared investigation, the ratio TeO_4/TeO_3 does not present important variations. One can suspect that, the stability of the Raman signal intensity associated to TeO_{3+1} and TeO_3 is a

Band position (cm^{-1})	Bandwidth (cm^{-1})
445	97
525	64
601	51
658	53
726	70
789	70
890	90

Figure 3. Magnitude of decomposed peak of Raman spectra in $80TeO_2$–$(20-x)TaO_{5/2}$–$xZnO$ glass systems. Desummation for the glass composition $80TeO_2$–$10TaO_{5/2}$–$10ZnO$ using the normalized Gaussian function $Ae^{-2\left[\frac{(v-v_0)}{w}\right]^2}$, ω the vibration band bandwidth, v_0 the vibration frequency.
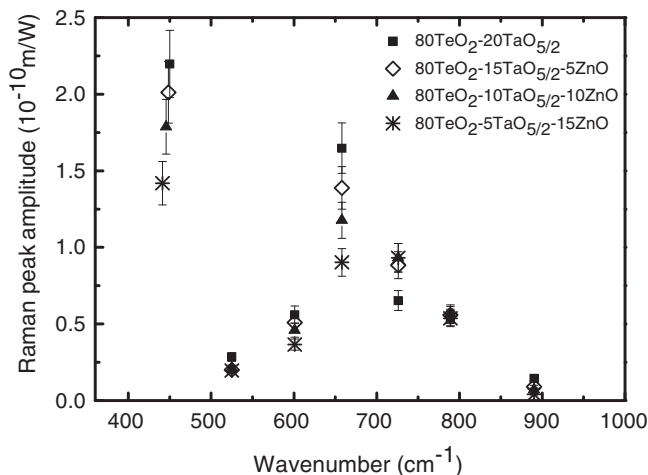
combined effect of an increase of the volume concentration of TeO_{3+1} or TeO_3 with a decrease of the Raman response of the TeO_n units.

All those observations are consistent with the fact that the substitution of tantalum for zinc results in a global decrease of the Raman cross section. These results indicate that it is not appropriate to solely correlate the magnitude of the vibrations to the volume concentration of the different TeO_n units. Rather, as stated above, a consideration of the Te networks' intermediate environment or middle range order need to be considered in the interpretation of spectra and resulting calculated gain. It is then reasonable to propose that the strong decrease of the Raman gain coefficient at around $450\,cm^{-1}$ and at $660\,cm^{-1}$ has to be related mainly to the dramatic decrease of the Raman cross section of the vibrations associated to Te–O–Te bridges and TeO_4 units.

As shown in the Figure 4, the area under the Raman spectra of the different glasses decreases by 25% as the zinc oxide is introduced. Since the Raman spectra depict mainly the TeO_n units, it indicates that a decrease of the Raman cross section of the tellurite network occurs, especially for the TeO_4 units. Miller et al. has mentioned that different parameters are responsible of a strong Raman intensity, such as angularly constrained bridged anions involving highly polarizable bonds with large bonds lengths [25].

The change of the vibrational response has to be related to a change of the environment of the TeO_n entities at the intermediate length scale. According to previous investigation, the decrease of Te–O–Te bridges and TeO_4 units lead to the formation of TeO_{3+1} or TeO_3 and to a depolymerization of the tellurite glass network. The evolution of the Raman response with the introduction of the zinc oxide results in a decrease of the area under the Raman spectra as shown in the Table 2. The magnitude of the Raman gain taken at $660\,cm^{-1}$ in the binary glass system is fairly constant, whereas in the ternary glass system, a drastic decrease of 50% is observed. This effect is mainly driven by the decrease of the Raman response associated to the TeO_4 disphenoids and the Te–O–Te bridges. One can expect that the introduction of zinc oxide leads to a depolymerization of the TeO_4 chain-like structure. Such depolymerization is supposed to affect the Raman response of the TeO_4 units. Soulis et al. and Mirgorodsky et al. [26,27] have proposed that the presence of chain-like structure leads to high polarizability and hyperpolarization of the tellurite network. Since the polarizability is affected by the depolymerization, one can propose that the Raman cross section should be also concerned. Based on such assumption, it seems that none only the volume fraction of the TeO_n units and the type of structural units have to be taken into account for the Raman gain but also the Raman cross section of the species which is affected by a change at the intermediate range scale. The introduction of zinc oxide has a major effect by the depolymerization of the tellurite network which modifies the ratio TeO_4/TeO_3 but also the local polarizability/hyperpolarizability and the Raman cross sections. It affects then the overall polarizability of the glass as proved by the linear index measurements depicted in Table 2.

In the glass studied, the Raman gain is related to the Raman response of the TeO_4 molecular entities. The direct relationship between Raman cross section and glass polymerization, intrinsically affects the value of the Raman gain. The ability of the ZnO for depolymerizing the tellurite network, leads to an important drop of the Raman response of the tellurite glasses.

5. Conclusion

A study based on the relationship between the glass structure and nonlinear optical property has been performed on the TeO_2–$TaO_{5/2}$–ZnO glass matrix by Raman and IR spectroscopies. TeO_2–$TaO_{5/2}$–ZnO represents a promising Raman gain medium (40 times higher than SiO_2) exhibiting a high stability against crystallization. This system has allowed demonstrating that the introduction of ZnO in tellurite glasses induces a decrease of the Raman cross section of the TeO_n structural units, mainly the TeO_4, due to a decrease of the Raman cross section. It has been shown that the Raman gains are related to the polymerization of the tellurite glass network. A more important decrease of the Raman gain has been observed in the ternary TeO_2–$TaO_{5/2}$–ZnO glass system than in the binary TeO_2–$TaO_{5/2}$ glass system. This difference has been related to the higher ability of ZnO for depolymerizing the tellurite network, than the $TaO_{5/2}$.

References

[1] R.N. Hampton, W. Hang, G.A. Saunders, R.A. El-Mallawany, Phys. Chem. Glasses 29 (3) (1988) 100.
[2] R. Stegeman et al., Opt. Express 13 (4) (2005) 1144.
[3] R. Stegeman et al., Opt. Lett. 28 (13) (2003) 1126.
[4] C. Rivero, R. Stegeman, M. Couzi, D. Talaga, T. Cardinal, K. Richardson, G. Stegeman, Opt. Express 13 (12) (2005) 4759.
[5] Sae-Hoon Kim, Toshinobu Yoko, Phys. J. Am. Ceram. Soc. 78 (4) (1995) 1061.
[6] C. Rivero et al., J. Appl. Phys. 101 (2007) 023526.
[7] I. Savelii et al., Opt. Mater. 33 (2011) 1661.
[8] S. Manning, H. Ebendorff-Heidepriem, T.M. Monro, Opt. Mater. Express 2 (2) (2012) 140.
[9] V.V. Safonov, V.N. Tsygankov, Physicochem. Anal. Inorg. Syst. 52 (12) (2007) 1991.
[10] G. Senhil Murugan, T. Suzuki, Y. Ohishi, Phys. Chem. Glasses 46 (4) (2005) 359.
[11] J. Lin, Z. Sun, C.S. Ray, D.E. Delbert, J. Non-Cryst. Solids 336 (2004) 189.
[12] E.I. Kamitsos, Y.D. Yiannopoulos, C.P. Varsamis, H. Jain, J. Non-Cryst. Solids 222 (1997) 59.
[13] E.I. Kamitsos, Phys. Rev. B 53 (1996) 14659.
[14] C. Rivero, K. Richardson, R. Stegeman, G. Stegeman, T. Cardinal, V. Rodriguez, J. Non-Cryst. Solids 345–346 (2004) 396.
[15] M.E. Lines, Phys. Rev. B 43 (1991) 11978.
[16] G. Dai, F. Tassone, A. Li Bassi, V. Russo, C.E. Bottani, F. D'Amore, IEEE Photonics Technol. Lett. 16 (2004) 1011.
[17] A.S. Pine, G. Dresselhaus, Phys. Rev. B 5 (1972) 4087.
[18] D.M. Korn, A.S. Pine, G. Dresselhaus, T.B. Reed, Phys. Rev. B 8 (1973) 768.
[19] A.P. Migrorodsky, T. Merle-Méjean, J.C. Champarnaud, P. Thomas, B. Frit, J. Phys. Chem. Solids 61 (2000) 501.
[20] J. Dexpert-Ghys, B. Piriou, S. Rossignol, J.M. Réau, B. Tanguy, J.J. Videau, J. Portier, J. Non-Cryst. Solids 170 (1994) 167.
[21] T. Sekiya, N. Mochida, A. Ohtsuka, M. Tonokawa, J. Non-Cryst. Solids 144 (1992) 128.
[22] M. Arnaudov, V. Dimitrov, Y. Dimitriev, L. Markova, Mater. Res. Bull. 17 (1982) 1121.
[23] O. Noguera, T. Merle-Mejean, A.P. Mirgorodsky, M.B. Smirnov, P. Thomas, J.C. Champarnaud-Mesjard, J. Non-Cryst. Solids 330 (2003) 50.
[24] N. Wada, M. Kubo, N. Maeda, M. Akira, K. Kojima, J. Mater. Res. 19 (2) (2004) 667.
[25] A.E. Miller, K. Nassau, K.B. Lyons, M.E. Lines, J. Non-Cryst. Solids 99 (1988) 289.
[26] M. Soulis, T. Merle-Mejean, A.P. Mirgorodsky, O. Masson, E. Orhan, P. Thomas, M.B. Smirnov, J. Non-Cryst. Solids 354 (2008) 199.
[27] A.P. Mirgorodsky, M. Soulis, P. Thomas, T. Merle-Mejean, Phys. Rev. B 73 (2006) 134206.